Peer-reviewed version available at *Land* **2020**, *9*, 305; doi:10.3390/land9090305

Sub-surface Carbon Stocks in Northern Taiga Landscapes Exposed in the Batagay Megaslump, Yana Upland, Yakutia

Andrei G. Shepelev[1,*], Alexander I. Kizyakov[2], Sebastian Wetterich[3], Alexandra M. Cherepanova[4], Thomas Opel[3], Loeka L. Jongejans[3], Jeremy Courtin[3], Alexander N. Fedorov[1,5], Hanno Meyer[3], Jinho Ahn[6], Igor I. Syromyatnikov[4], Grigoriy N. Savvinov[7]

[1] Laboratory of Permafrost Landscapes, Melnikov Permafrost Institute, Siberian Branch of the Russian Academy of Science, 36 Merzlotnaya St., 677010 Yakutsk, Russia; carbon-shag@yandex.ru
[2] Cryolithology and Glaciology Department, Faculty of Geography, Lomonosov Moscow State University, GSP-1, Leninskie Gory, 119991 Moscow, Russia; akizyakov@mail.ru
[3] Alfred Wegener Institute, Helmholtz Centre for Polar and Marine Research, Telegrafenberg A45, 14473 Potsdam, Germany; sebastian.wetterich@awi.de, thomas.opel@awi.de, loeka.jongejans@awi.de, jeremy.courtin@awi.de, hanno.meyer@awi.de
[4] Laboratory of General Geocryology, Melnikov Permafrost Institute, Siberian Branch of the Russian Academy of Science, 36 Merzlotnaya St., 677010 Yakutsk, Russia; alexandra_587@mail.ru, igor@mpi.ysn.ru
[5] Biogeoscience Educational and Scientific Trainings, North-Eastern Federal University, 677000 Yakutsk, Russia; anfedorov@mpi.ysn.ru
[6] School of Earth and Environmental Sciences, Seoul National University, Seoul 151-742, Republic of Korea; jinhoahn@gmail.com
[7] Science Research Institute of Applied Ecology of the North, North-East Federal University, 43 Lenin Avenue, 677007 Yakutsk, Russia; g.n.savvinov@mail.ru
* Correspondence: carbon-shag@yandex.ru; Tel.: +7-914-265-89-79

Abstract: The most massive and fast-eroding thaw slump of the Northern Hemisphere located in the Yana uplands of northern Yakutia was investigated to assess in detail the cryogenic inventory and carbon pools of two distinctive Ice Complex stratigraphic units and the uppermost cover deposits. Differentiating into modern and Holocene near-surface layers (active layer and shielding layer), highest total carbon contents were found in the active layer (18.7 kg m^{-2}), while the shielding layer yielded much lower carbon content of 1.8 kg m^{-2}. The late Pleistocene upper Ice Complex contained 10.4 kg m^{-2} total carbon, and the mid-Pleistocene lower Ice Complex 17.7 kg m^{-2}. The proportion of organic carbon from total carbon content is well above 70% in all studied units with 94 % in the active layer, 73% in the shielding layer, 83% in the upper Ice Complex and 79% in the lower Ice Complex. Inorganic carbon is low in the overall structure of the deposits.

Keywords: Ice Complex; Yedoma; organic carbon; inorganic carbon; total carbon; Batagay megaslump; North Yakutia

1. Introduction

Pioneering fieldwork in the Batagay megaslump to study its cryogenic inventory and origin was undertaken in 2011 [1]. The prominent ice-rich ice complex units and ice-poor sand units as well as enclosed ground ice exposed in the Batagay megaslump accumulated during the Pleistocene under the continental conditions of the non-glaciated region of eastern Siberia belonging to the western part of Beringia [1].

Currently, the Batagay megaslump and its exposed permafrost are increasingly studied by various disciplines to assess its modern morphodynamics such as erosion rates and budgets [2, 3] or the behaviour of living microorganisms inside the frozen zone [4]. Most studies, however, deal with the Quaternary frozen deposits, the fossil inventory and ground ice.

Based on current cryolithological research and various dating approaches the permafrost exposed in the Batagay megaslump differentiates into the following seven units [1, 5, 6] starting from the slump bottom: (1) diamicton above slate bedrock, (2) lower ice complex, (3) lower sand unit, (4) prominent lenses of woody debris, (5) upper ice complex, (6) upper sand unit, and (7) a near-surface layer. The chronological sequence is not continuous, but contains hiatuses and traces of thermo-erosional degradation, especially during multiple interglacials during mid- and late Pleistocene [6–8].

Geophysical studies and obtained data on the general permafrost structure of the Batagay megaslump show – as also in the headwall of the slump exposed – multiple wedge-ice generations. These are thickest on the northwestern slope of megaslump, and thinnest on the south and southwest slopes. The distance between the ice wedges ranges from 2 to >10 m [9].

The analysis of stable water isotope ($\delta^{18}O$, δD) composition of the ice wedges from the upper ice complex revealed low winter temperatures during MIS 3 under enhanced continentality of the Yana Upland [5, 10]. Ice wedges of both sand units retain traces of rapid sand formations [5]. It was further shown that the wedge ice of multiple generations of the Batagay megalump has a hydrogencarbonate-calcium dominated composition and a homogenous content of micro- and macroelements [11] pointing to stable moisture sources, i.e. winter precipitation, for syngenetic ice wedge growth.

The reconstruction of past vegetation and landscapes of the Yana Upland indicated that the primary plant, formed in cold stages before and after the Last Interglacial, corresponds to the analogues of moderately dry meadow steppes represented by *Festucetalia lenensis* communities [12]. During the last interglacial period, larch was the main vegetation, and coniferous forest corresponded to modern northern taiga [8]. The meadow steppes that formed the vegetation cover during the cold periods retained their ecological properties even under warm stage conditions of the Last Interglacial, which indicates environmental stability over glacial-interglacial cycles. Such ecological balance means a low amount of precipitation and a relatively mild growing season during and after the late Pleistocene. The studied ancient vegetation proxies are relics of a continuous steppe system, stretching from Central Siberia to Northeastern Yakutia in the Pleistocene [12].

Research and analysis of the carbon of fossil organic matter in permafrost sediments are needed because of the ongoing climate warming and increasing anthropogenic load on sensitive ecosystems of permafrost landscapes. Whether its economic or industrial development, which leads to impaired ecological stability. As a result, exogenous and cryogenic processes are activated with higher intensity leading to the formation of depressions in the landscape, melting of ground ice, active layer thickening and the inevitable loss of the once stable part of carbon. For example, fires and clear-cutting of forests adversely affect the state of permafrost [13]. It shows that ten years after continuous forest cutting, the soil temperature rose by 1°C, and the thickness of the active layer increased to about 2 m, which led to a critical state of permafrost [13]. After 60–80 years, gradual self-healing of permafrost landscapes takes place, the thickness of the active layer decreases, and secondary birch-larch forests grow. Studies [14] indicated that, after the cessation of the pyrogenic situation and the burning of all forest vegetation for about 20 years, direct sunlight penetration causes thickening of the seasonal thaw depth. Still, the gradual restoration of flora and the accumulation of peat layer initiates the reverse process and leads to a decrease of the seasonal thaw depth.

Cover deposits and underlying permafrost are a planetary reservoir of carbon (of any form) since its accumulation took place over long geological periods. Carbon preserved in the permafrost is represented by various labile fractions such as humus-like and humus compounds, as well as dissolved organic substances. However, in scientific practice,

Peer-reviewed version available at Land 2020, 9, 305; doi:10.3390/land9090305

researchers use the total carbon content to assess, predict and model ecosystem changes under the influence of permafrost degradation or aggradation. About 70% of carbon in the terrestrial ecosystems of the Earth is accumulated in soils amounting to 1395–1580 Gt C. Of this carbon stock, 14% belong to soils of tundra and forest-tundra zones and 13% to those of boreal (taiga) forests [15–17].

Geographically, the northern taiga forests of Northern Yakutia are isolated by the Verkhoyansk Mountains. A comprehensive analysis of the carbon content and stock in continental permafrost deposits is lacking yet, and the existing scientific data is scarce. Estimates of organic carbon stocks in the northern taiga amount to about 16 to 22 kg m^{-2} in the uppermost 1-metre-thick soil layer [18], while 30 to 50 kg m^{-2} of organic carbon are stored in the uppermost 3 meters of permafrost on a circum-arctic scale [19].

The carbon component in the landscapes of the circumpolar region is one of the criteria for observing the influence of anthropogenic and natural factors on permafrost. Changes occurred in the violation of pristine properties of the soil cover entail the inevitable loss of carbon from the active layer and permafrost as CO_2, CH_4 and physical removal by erosion into riverine and marine realms. The permafrost exposed in the Batagay megaslump is an important example of how natural permafrost feature experiences overall degradation, changing as a result of human activities, the geological structure of the territory and due to its geographical location. However, according to Masyagina and Menyailo [20], the permafrost of Siberia will remain stable soon, but it is still a potential source of a vast amount of greenhouse gases, and ongoing release into the atmosphere will result in a further temperature increase, which is the permafrost carbon feedback.

In our study, we provide a detailed cryolithological description of the permafrost units exposed in the Batagay megaslump. We further estimated the carbon stocks of the lower and upper ice complex as well as the uppermost cover layers.

2. Study area

The climate of the Yana upland region is severe and sharply continental. It is affected by the geographical location between the arctic and subarctic climatic zones as well as by isolation between mountain ranges. The average air temperature in January ranges from –40 to –38 °C, and the average air temperature in July from about +14 to +16°C. The average annual rainfall with 180–200 mm is low – comparable to those of deserts and semi-deserts [21].

The vegetation of the northern taiga is characterized by low species diversity, in mountain climates with predominantly insufficient atmospheric moisture. In the study area, forests are dominated by larch (*Larix cajanderi*) with undergrowth of birch, cedar dwarf pine, lingonberry, and moss-lichen communities [22]. Landscapes are formed on permafrost in continuous distribution with mean annual ground temperatures from –7 to –4°C. In the Verkhoyan-Kolyma region, the maximum permafrost thickness reaches 350 m depth [23]. The presence of ice-rich permafrost in combination with widespread cryogenic processes such as thermokarst, thermo-erosion, solifluction and frost cracking, determine the appearance of periglacial landscapes and their development.

The loose deposits in the area are underlain by a bedrock of the Triassic age of the Ladinsky tier such as sandstones, siltstones and conglomerates. Quaternary formations are represented by undivided frozen eluvium and diluvium consisting of sand, silt and clay including ground ice and organic matter.

3. Materials and methods

Preprints (www.preprints.org) | NOT PEER-REVIEWED | Posted: 22 July 2020 doi:10.20944/preprints202007.0525.v1

Peer-reviewed version available at Land 2020, 9, 305; doi:10.3390/land9090305

During fieldwork in March-April 2019, the thaw slump walls were sampled at four locations (Figure 1 and Figure 2). The sampled stratigraphic units exposed in the wall of the slump are marked as follows: A1 (lower Ice Complex), B1 (upper Ice Complex) close to the headwall of the slump, D1 (ravine) in the south-facing exposure and C1 (upper Ice Complex) in the north-facing exposure (Figure 1). Firstly, the walls of the sections were carefully cleaned to remove the outermost material in order to avoid contamination. Secondly, the sampling profiles were cryolithologically described in detail. Finally, we took samples of the stratigraphical horizons for carbon analysis and soil density calculations. The soil density (g m^{-3}) in natural composition was determined by taking samples every 10 cm into steel cylinders with a defined volume of 100 cm^3. Knowing the mass of the cylinder with soil and the mass of the empty cylinder, we determined the difference in soil mass at certain moisture content. By determining the moisture percentage, we calculated the dry mass of the material. The density of the soil of undisturbed composition was obtained by dividing the mass of dry soil by cylinder volume.

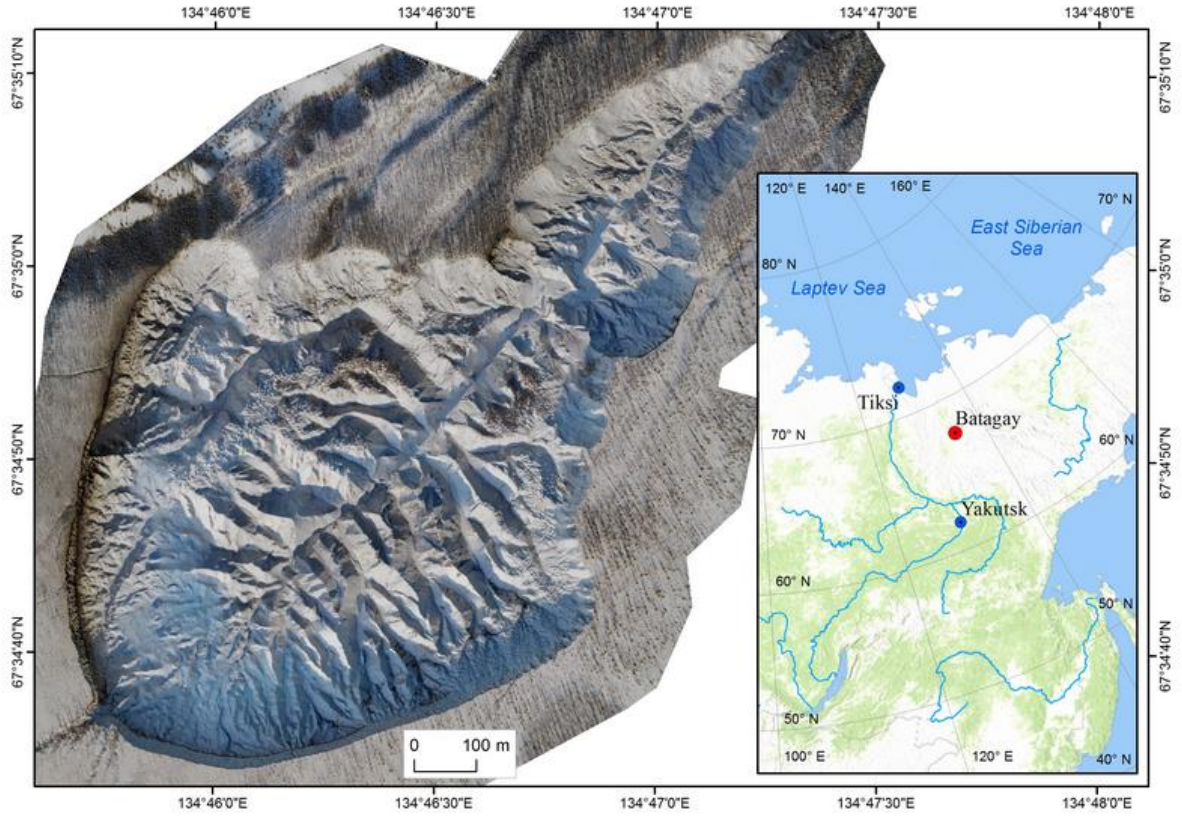

Figure 1. Batagay megaslump location in the Yana Upland in Northeast Yakutia and orthophotomosaic overview based on unmanned aerial vehicle (UAV) data from April 2019.

The soil samples were processed in the laboratory at room temperature. The sediment was laid out on paper and dried to an air-dry state. After that, the samples were oven-dried for 10 hours at a temperature of 105°C to exclude excess moisture from the samples.

We determined the organic carbon (OC), inorganic carbon (IC) and total carbon (TC) content using a certified LECO RC612 multiphase carbon analyzer, according to DIN19539. The applied temperature programming allows dividing the various carbon forms into organic and inorganic. The maximum temperature for burning samples was 1100°C in an oxidizing atmosphere.

Carbon stocks (kg m^{-2}) were calculated for each selected layer. We calculated the stocks for the active and shielding layers and underlying permafrost and summed them to get the total carbon stock for the entire thickness. The calculation of carbon stocks was carried out, according to the equation:

$$\text{Eq.: } S = H \times p \times X,$$

where S – carbon stock (kg m^{-2}), H – soil layer depth (cm), p – soil density (g m^{-3}) and X – average carbon content (%).

Statistical processing of the carbon data was carried out in the program StatSoft STATISTICA for Windows 13.3. To exclude distorted indicators in the sample set, a typical sample from the general set of observations was used. The data are presented as arithmetic means with the standard error of the mean values.

4. Results and discussion

4.1. General cryostratigraphy of permafrost exposed in the Batagay megaslump

The Batagay megaslump is the largest one in the Northern Hemisphere occupying an area of 81 hectares, and with a length of more than 1000 m and a width of 800 m in 2019 (see Figure 1 and Figure 2). The slump expands at high rates along the perimeter of up to 0.026 km^2 $year^{-1}$ (between 1991 and 2018) [3]. The exposed depth along the slump perimeter varies depending on the ice content of the permafrost deposits and the activity of thermo-erosion. It reaches up to about 60 m depth in the central part of the headwall. The slope inclination is pre-defined by exogenous geological processes that formed the slopes of the adjacent Kirgilyakh and Khatyngnakh mounts, subsequent long-term aggradation of partly very ice-rich permafrost, i.e. Ice Complex, and thermo-erosion along with valley structures on the slopes by ground ice melt. The Batagay megaslump morphodynamics is characterized by active thermo-erosion at the walls and the fluvial erosion by temporary streams on the slump bottom. The latter transports eroded fine material with meltwater along the central slump channel into the floodplain of the Batagay River. However, substantial amounts of the eroded material, as well as permafrost remnants, remain on the slump bottom, forming a high relief of ridges and hills with different heights (Figure 2).

Preprints (www.preprints.org) | NOT PEER-REVIEWED | Posted: 22 July 2020 doi:10.20944/preprints202007.0525.v1

Peer-reviewed version available at Land 2020, 9, 305; doi:10.3390/land9090305

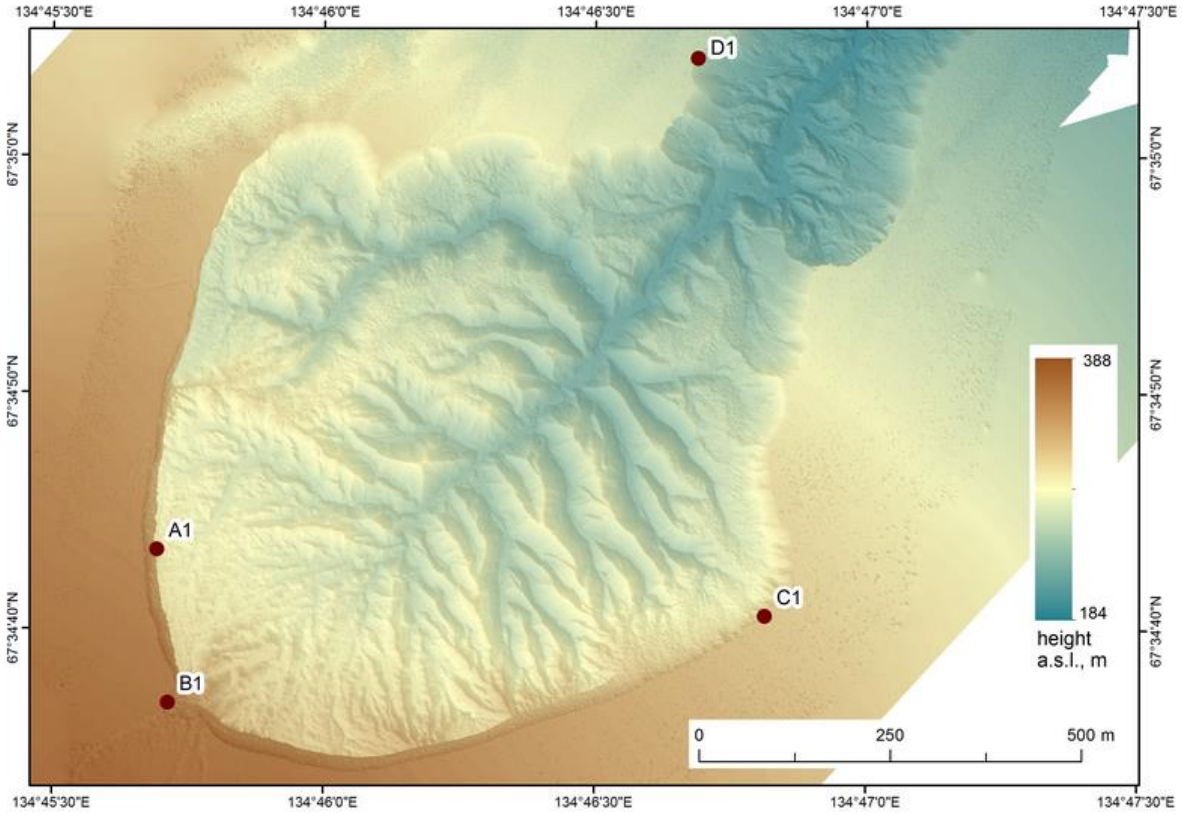

Figure 2. Digital Surface Model (DSM) based on UAV data from April 2019. Sampling locations: the lower ice complex (A1), the upper ice complex (B1, C1) and cover deposits in the ravine (D1).

The stratigraphy in the southern exposure of the slump – close to the central headwall (sampling points A1 and B1) – was characterized by the lower and the upper Ice Complex units (about 3–7 m and 20–25 m thick, respectively), separated by the lower sand unit (up to about 20 m thick) and a distinct woody bed (up to about 3 m thick) at the base of the upper Ice Complex (Figure 3 and 4). The upper Ice Complex was covered by the uppermost sediment layer with a thickness of 1.5 m.

Ice wedges of the upper Ice Complex were distributed to a depth of 14–24 m from the top of the slump. The upper Ice Complex contained many thin plant roots as well as large fragments of tree trunks. Below the upper Ice Complex at a depth of about 23 m, a sandy loam layer with an admixture of reddish-orange sand with a thickness of 1 m was striking. Underneath this layer with a thickness of 1.5–2.0 m, there was an organic-rich layer with numerous plant and wood fragments of different degrees of decomposition (woody bed; Figure 4). From a depth of 26 m lied a sandy loam of grey and light brown colour with narrow veins of sand of orange colour with narrow composite wedges and many thin roots (lower sand unit). There were brown organic residues with a pungent odour of rotting material, as well as visible individual inclusions of charcoal.

Preprints (www.preprints.org) | NOT PEER-REVIEWED | Posted: 22 July 2020 doi:10.20944/preprints202007.0525.v1

Peer-reviewed version available at Land 2020, 9, 305; doi:10.3390/land9090305

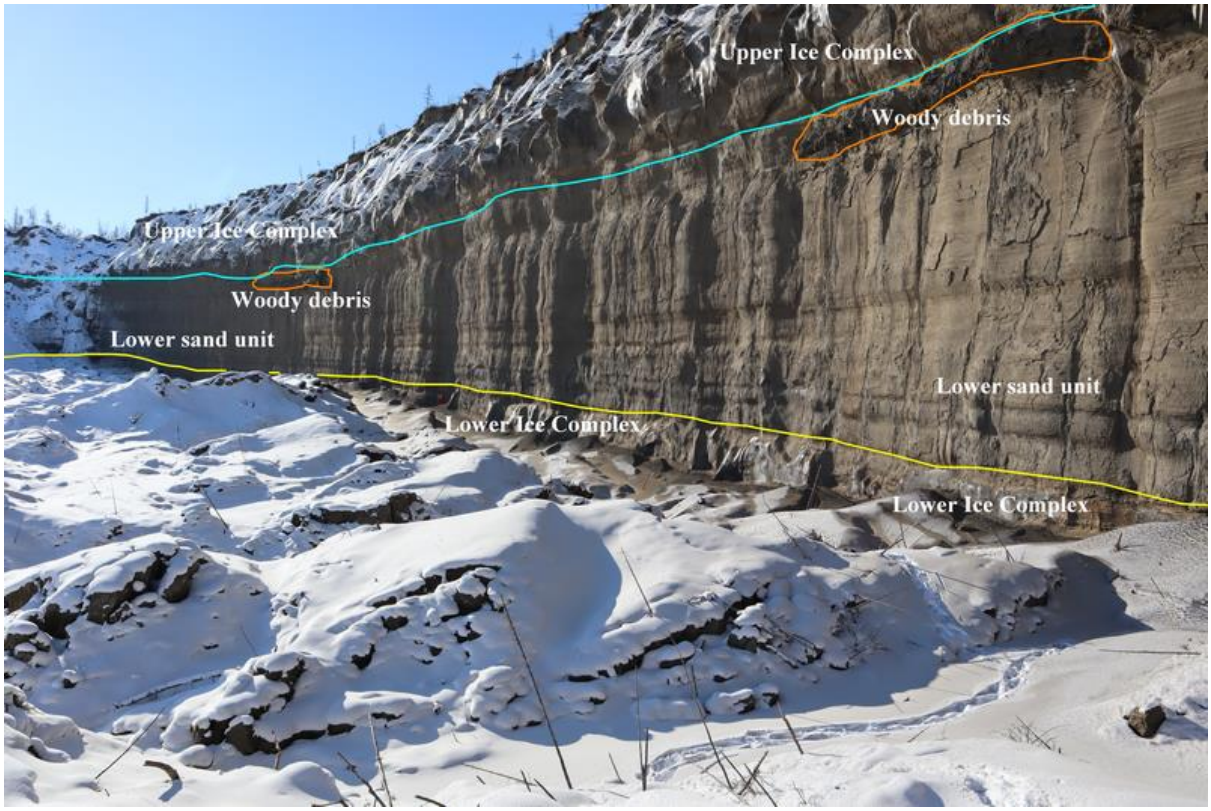

Figure 3. Outcrop in the form of a steep wall (southern exposure), represented by upper and lower ice complex units intersected by the lower sand unit and overlain by the shielding and active layers.

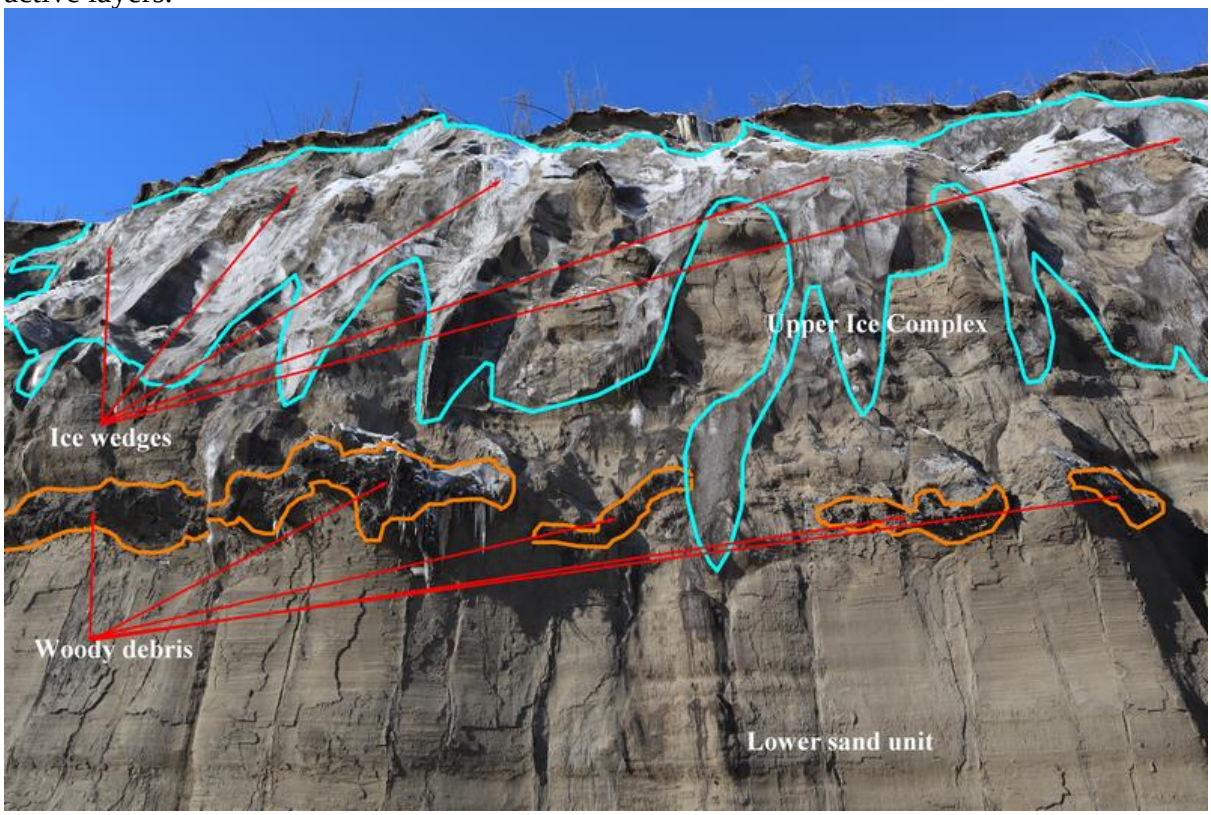

Figure 4. The upper Ice Complex unit overlying the woody bed (orange line) and the lower sand unit.

Preprints (www.preprints.org) | NOT PEER-REVIEWED | Posted: 22 July 2020 doi:10.20944/preprints202007.0525.v1

Peer-reviewed version available at Land 2020, 9, 305; doi:10.3390/land9090305

The lower sand unit ended at a depth of 51 m and had a thickness of 25 m. Between the depths of 51 and 52 m, there was a layer of reddish-orange sand with a thickness of 0.4–0.5 m. From the depth of 51.5 m, the lower Ice Complex began with a thickness of up to 6–7 m. The upper boundary (visible part) of the ice wedges had a height of 0.4–1.2 m. There were ice schlieres with angled direction from the sides of the ice wedges. Above the ice wedges, there was a layer consisting of icy sandy loam of dark grey colour which was penetrated by roots, and below lied a layer of silty sandy loam of brown colour alternating with crushed stones, inclusions of charcoal and narrow strips of peat.

The wedge ice of the upper Ice Complex was pillar-shaped, resembling a solid wall of ice from a distance. Table 1 summarizes descriptions of the cover deposits (samples in profiles B1, C1 and D1) of the upper Ice Complex, mainly composed of sandy and dusty particles with localized separate newly formed structure (ironing) and individual mechanical inclusions of pebbles and gravel, they form one soil pedon for the Batagay megaslump. The unit sampled at A1 represents a separate feature of the lower Ice Complex. The formation of the lower Ice Complex and its preservation remains uncertain. Perhaps, the lower Ice Complex survived at least partly due to the thick and rapidly accumulated lower sand unit up to about 25 m thick that is relatively ice-poor. But in this case, what contributed to such an active accumulation of sedimentary cover over the lower Ice Complex? The lower Ice Complex is surrounded by a heterogeneous composition of material such as sandy loam and loess. The origin and existence of loess to a depth of 58 m suggests the accumulation of loess formations occurred as a result of frost weathering and solifluction processes due to periglacial phenomena in the Batagay area.

Table 1. Cryolithological characterization of the studied stratigraphic features exposed in the Batagay megaslump.

Sampled units	Description of selected profile sections
A1. Lower Ice Complex, southern exposure: N67°34'43,35" E134°45'41,58"	At the top there are light brown layers of loess with streaks of organic residues and hanging thin root. Single inclusions of coal are present. The width of the interlayers varies from 0.15 to 0.35 m. At the height of 1.5–1.7 m from the bottom of the slump, there is a strip of gravel of 1.2 m long. The size of the gravel varies from 3 mm to 3.5 cm. The profile is homogeneous; it is composed of sandy loam (sandy and dusty particles) of a dark grey colour. The horizon is riddled with rare roots. There are inclusions of charred wood residues – small inclusions of brown decomposed organic matter. To the right of the sampling site, at a distance of 1.6 m and a height of 1.5 m, there is a light-brown interlayer with an orange tint of about 2.1 m long and 0.4 m wide. Its structure consists of small lumps with a diameter of 0.1-0.5 mm. Spots of black coal and thin roots are observed. In some sections, the material contains alternating ice schlieren. It has a conditional ataxic cryostructure. Above the interlayer, dark grey sand contains many roots.
B1. Upper Ice Complex, southern exposure: N67°34'36,87" E134°45'42,84"	Section from top to bottom at the edge of the wall: 0.0–0.04 m – forest litter (mosses, lingonberries, needles, rags). 0.04–0.14 m – humus horizon. 0.14–0.25 (0.30) m – light brown sandy loam with inclusions of coal, strongly penetrated by roots. 0.25 (0.30)–1.2 m – dark grey sandy loam, transition to the next horizon is clear, the border is even. The horizon contains many thin

	roots. The texture of the horizon is homogenous, with the exception of crushed stone inclusions at a depth of 0.8 m. 1.2–1.5 m – grey sandy loam with a whitish tint, a row of gravel separately located at a distance of 0.04 to 0.1 m, diameter from 0.002 to 0.01 m. 1.5 m – permafrost of the upper ice complex.
C1. Upper Sand, northern exposure: N67°34'40,58" E134°46'48,86"	Section from top to bottom from the edge of the wall: 0.0–0.03 m – forest litter (mosses, lingonberries, needles, and rags). 0.03–0.08 m – dark brown humus horizon. 0.08–0.39 m – loam of light brown colour, containing many roots. The transition to the next horizon is noticeable, the border is even, there were inclusions of pebbles with a diameter of 70–90 mm. 0.39–1.01 m – dark brown sandy loam. At a depth of 0.39–0.53 m, a large accumulation of roots from 0.53 m. At a depth of 0.74 m, there are holes with a diameter of 2 cm. The texture of the horizon is homogeneous.
D1. Ravine, southern exposure: N67°35'04,16" E134°46'41,34"	Section from top to bottom from the edge of the wall: 0.0–0.02 m – forest litter (leaves, needles, rags). 0.02–0.09 m – dark brown humus horizon, roots of different diameters abundant. 0.09–0.29 m – silt sandy loam of light brown colour strongly penetrated by roots. The transition to the next horizon is subtle, the border is smooth. 0.29–1.0 m – grey sandy loam, rare thin roots, the horizon is homogeneous.

4.2. Carbon stocks of the lower and the upper Ice Complex units, and the uppermost cover

It is necessary to take into account that microorganisms begin to multiply actively in thawing permafrost [20]. When organic matter is oxidized, they remove carbon from the bound state into the atmosphere. The degree of decomposition of soil organic matter depends on the properties of the soil, the depth of the profile and community of bacteria, archaea and eukaryotes, which are mostly found in frozen soils. This will lead to the intensification of microbial metabolic activity and the possible creation of positive feedback to the conditions of anticipating thawing of the permafrost [24–27].

The main fraction of OC was concentrated in the active layer topping the upper Ice Complex due to the productivity of this layer, both in terms of greater seasonal thawing and processing of soil organic matter by microbes (Table 2).

The resulting determinants are soil warming up to positive temperatures and activation of microbiological processes; as a result, destruction and intensive mineralization of animals and plant residues occur. Variations in the OC content in the active layer varied widely from a minimum value of 0.3% to a maximum of 12.5%. Higher content of OC was prevalent on the slopes of the southern exposure. Consequently, for the northern exposure slope (C1), the average OC value was 2.1%, while for the southern exposure (B1) and the ravine (D1) it was higher with 3.5% and 2.8%, respectively. The deep penetration of heat on the southern exposure slopes causes permafrost thaw and collapse in the warm period of the year compared with the northern exposure slopes, as is noticeable in the picture (see Figure 1). This increases the physical runoff of soil material into the Batagay River as well as its subsidence on the bottom of the slump.

Preprints (www.preprints.org) | NOT PEER-REVIEWED | Posted: 22 July 2020 doi:10.20944/preprints202007.0525.v1

Peer-reviewed version available at Land 2020, 9, 305; doi:10.3390/land9090305

The properties of the shielding layer are closely related to the active (seasonally thawed) layer. The susceptibility of the seasonally thawed layer to the constant cycle of freezing and thawing determines the presence or absence of the frozen shielding layer at the uppermost part of permafrost. In case of destruction of the vegetation cover, the active layer degrades as a result of soil temperature increase, and the shielding layer loses its usual boundaries and merges with seasonally thawed soil, which leads to a lack of shielding properties leading to permafrost degradation and thaw subsidence. The average OC content in the shielding layer was low if compared to the active layer, reaching only 0.3%. This low OC content is most likely due to the buffer properties of the shielding layer, its low thickness, low moisture content, and the paretic rate of chemical reactions. In the permafrost layer, the average OC content for the lower Ice Complex (A1) was 0.65% and for the upper Ice Complex (B1) is 1.04%. There was a concentration increase of 58.5% and 74.0% compared to the shielding layer. Perhaps this is the result of the genetic features of lower cryogenic horizon formation and the water presence in it with ongoing metabolic processes even at temperatures below 0°C. It is worth noting that in the past, organic residues deposited in combination with heterotrophic microbial activity, are capable of carbon remineralizing despite the negative temperature of the deposits.

Table 2. The carbon content in the cover deposits of the upper and lower Ice Complex units. SD – standard deviation, min – minimum value, max – maximum value, mean – mean value, OC – organic carbon, IC – inorganic carbon, TC – total carbon.

B1. Upper Ice Complex. Southern exposure of the slump				
Index	Unit	OC, %	IC, %	TC, %
min	Active layer	0.27	0.06	0.36
max		12.49	0.59	13.07
mean		3.50	0.23	3.74
SD		*1.62*	*0.08*	*1.70*
min	Shielding layer	0.26	0.09	0.36
max		0.27	0.11	0.38
mean		0.27	0.10	0.37
SD		*0.01*	*0.01*	*0.01*
min	Upper Ice Complex (permafrost)	0.71	0.21	0.92
max		1.38	0.23	1.60
mean		1.04	0.22	1.25
SD		*0.14*	*0.01*	*0.14*
A1. Lower Ice Complex. Southern exposure of the slump				
min	Lower Ice Complex (permafrost)	0.52	0.14	0.68
max		0.89	0.20	1.08
mean		0.65	0.17	0.82
SD		*0.03*	*0.01*	*0.03*
C1. Upper Ice Complex. Northern exposure of the slump				
min	Active layer	0.34	0.08	0.45
max		6.85	0.32	7.13
mean		2.05	0.15	2.20
SD		*0.79*	*0.03*	*0.81*
D1. Ravine. Southern exposure of the slump				
min	Active layer	0.27	0.10	0.38
max		8.98	0.30	9.28

Preprints (www.preprints.org) | NOT PEER-REVIEWED | Posted: 22 July 2020 doi:10.20944/preprints202007.0525.v1

Peer-reviewed version available at Land 2020, 9, 305; doi:10.3390/land9090305

mean		2.77	0.16	2.92
SD		*0.98*	*0.02*	*1.00*

The deposits of the Batagay megaslump had a small amount of carbonate in their composition. This is apparent in low inorganic carbon values, and there were no significant variations over depth. The inorganic carbon distribution was homogeneous both in the active layer and permafrost with systematic low values over the entire profile of sediments. Consequently, oxide group of minerals took part in the formation of the deposits, for example, quaternary formations of the slump mainly consisted of quartz minerals in the form of sand and they are represented by the loess fraction.

The TC content is formed from the two previous fractions, so, for the most part, it repeats the nature of distribution in the differentiated layers and the equivalent total content in the deposits.

Table 3 shows the carbon stocks of the studied stratigraphic features of the Batagay megaslump. The enormous amount of organic carbon was stored in the active layer for sections B1 and D1, where 60% of organic carbon was concentrated. At the same thickness of the active layer, the OC in C1 amounted to 9.5 kg m^{-2}, while the OC of D1 reached 18 kg m^{-2}, which was almost twice as much. Even with a changing of slope exposure the stocks for these sections in the active layer increased from the northern to the southern exposure by 42%–47% of organic carbon.

Table 3. Carbon stocks of different facies features of the Batagay megaslump.

B1. Upper Ice Complex. Southern exposure of the slump				
Depth, m	Unit	OC, kg m^{-2}	IC, kg m^{-2}	TC, kg m^{-2}
0.04–0.14	Active layer	11.23	0.63	11.85
0.14–0.25(0.30)		1.25	0.16	1.41
0.25(0.30) –1.2		4.03	1.42	5.45
SD		*1.56*	*0.18*	*1.60*
1.2–1.5	Shielding layer	1.31	0.50	1.81
SD		*0.01*	*0.02*	*0.03*
1.5–2.0	Upper ice complex (permafrost)	8.53	1.81	10.35
SD		*1.13*	*0.03*	*1.12*
Total		27.48	4.55	32.00
SD		*1.02*	*0.16*	*1.11*
A1. Lower Ice Complex. Southern exposure of the slump				
58.4	Lower ice complex (permafrost)	1.08	0.26	1.34
58.8		3.27	0.76	4.03
59.1		2.70	0.96	3.66
59.6		7.03	1.60	8.63
Total		14.08	3.58	17.65
SD		*0.58*	*0.13*	*0.71*
C1. Upper Ice Complex. Southern exposure of the slump				
0.0–0.03	Active layer	2.26	0.10	2.36
0.03–0.08		0.70	0.07	0.77
0.08–0,39		1.81	0.54	2.35
0.39–1.01		4.75	1.26	6.01
Total		9.51	1.97	11.48
SD		*0.45*	*0.15*	*0.58*

Preprints (www.preprints.org) | NOT PEER-REVIEWED | Posted: 22 July 2020 doi:10.20944/preprints202007.0525.v1

Peer-reviewed version available at Land 2020, 9, 305; doi:10.3390/land9090305

D1. Ravine. Northern exposure of the slump				
0.02–0.09	Active layer	6.65	0.21	6.86
0.09–0.29		6.51	0.40	6.92
0.29–1.0		4.87	1.36	6.23
Total		18.03	1.97	20.01
SD		*0.44*	*0.17*	*0.38*

The lowest carbon stocks of all studied stratigraphic features were recorded in the shielding layer, reaching 1.3 kg OC m^{-2} and 0.5 kg IC m^{-2}. IC stocks in the active layer of section B1 did not differ from the other two profiles (C1 and D1) and ranged from 2 to 2.2 kg m^{-2}. Carbonates enriched the first meter from the surface in non-permafrost soils. Under permafrost conditions, rather high inorganic carbon data were observed, 1.8 kg m^{-2} close to the level of the active layer. Section A1 had a higher IC stock of 3.6 kg m^{-2}. By moving to the lower ice complex, the IC reserves were in an inactive state due to the influence of negative soil temperature, substances trying to penetrate with soil solutions to the Yedoma horizons, and most likely the reserves remained unchanged for an extended period. Low estimates of inorganic carbon in the deposits of the Batagay slump are the result of low natural carbonate, as well as frosty weathering of rocks. Carbonate formation occurs in soil pores and frost cracks, indicating their predominant dissolution and leaching in conditions of cold climate.

In the upper two meters of the Ice Complex, carbon stocks were 32 kg m^{-2}. In the study area, the dominating forest species is *Larix cajanderi*. Its phytomass reserves barely exceed 6.0 kg m^{-2}, which is formed mainly due to green, lignified aerial parts, roots and moss-lichen complexes. Stocks of dead organic matter are 3 kg m^{-2}, and litter is 2.5 kg m^{-2}. In the northern taiga zone they are considered the forests with the lowest production about 11.5 kg m^{-2} per year [28]. As a result, carbon accumulation rates are low in the sediments of the upper Ice Complex. The main part of the organic matter is stored on the surface as a humus horizon of the soil, which undergoes degradation and weak decomposition, and the mineralization rate in such natural conditions remains low.

Permafrost degradation caused by global warming is not always a catastrophic consequence for the ecumene. To justify this point of view, we give a few well-founded examples. Siberian larch forests occupy 40% of all coniferous wood in Russia, which develop on permafrost. The amount of accessible nutrients for trees increases with permafrost degradation, which causes an increase in their biomass [29]. An increase in the average annual temperature and rainfall contributes to the advancement of natural zones deep into the north, expanding the agricultural area and changing the structure of the soil cover with an increasing share of organic matter due to an increase in the productivity of vegetation [30].

The permafrost zone has changed repeatedly, giving way to periods of warming and cooling, which favoured the formation and accumulation of permafrost in the past. With a certain degree of probability, it can be assumed that the multi-tiered features of the Batagay megaslump and their heterogeneous origin are the results of the participation of several geological factors:

(a) prolonged permafrost conditions of the territory with cryogenic and exogenous processes occurring in it;

(b) the transfer of aeolian material and its accumulation;

(c) the movement and deformation as a result of the tectonic influence of the territory;

(d) the impact of the Quaternary climate and paleoclimate.

6. Conclusions

In Yedoma deposits, carbon stocks are at a low level, typical of Northern Yakutia. The potential for the formation of organic matter in the local natural conditions of the Yana upland is limited by climatic features and primary production of the forest. First of all, the soft parts of plants and carbon fractions readily accessible to microorganisms decompose to the final mineralization product, and the bulk of the organic matter reserves are stored on the soil surface, forest litter and in the first meter of the Ice Complex. As long as these reserves remain intact, the organic system is in a stable state, and there is a dynamic equilibrium between the release of carbon and its decrease in the atmosphere.

The upper Ice Complex (B1) shows the distribution of the carbon in the elementary layers and the conjugation of carbon from the thickness and the amount of carbon available for mobilization in them. The maximum reserves of total carbon are contained in the active layer and amount to 18.7 kg m^{-2}, the minimum in the shielding layer is 1.8 kg m^{-2}, and in permafrost rocks, it is 10.4 kg m^{-2}. In total, 32 kg m^{-2} was deposited in a two-meter thickness. The ratio of organic and inorganic carbon in the section varies in scale for the active layer – 15, the shielding layer – 3 and permafrost deposits – 5. The ratio indicators show that organic carbon is the dominant feature in the soil horizon, layer or sediment. The higher this value, the more organic part is contained in a particular element of the Ice Complex. Also, this indicates the ability of organic carbon to be a nutrient medium for microorganisms and a source of CO_2. Inorganic carbon indicates the level of carbonate in a given horizon.

There is no doubt that the continental [1, 6] genesis of the formation of the lower Ice Complex (A1) and its archaic past, compared with the upper Ice Complex (B1), affected the loss, impossibility of renewal and accumulation of plant organic matter. The cycling of the biogenic elements was interrupted by the rapid accumulation of sandy loam layers and sediment deposits [5] and most likely the removal of organic layer beyond the meadow steppes [31] due to aeolian processes. We estimated the amount of ancient buried carbon at 17.7 kg m^{-2} for a thickness of 1.2 m.

Acknowledgement

We are grateful to the researchers of the Institute of Applied Ecology of the North of North-East Federal University, Yakutsk for providing the opportunity to research the Batagay thaw slump. We are sincerely grateful to the rescuer and climber of the Ministry of Emergency Situations of Russia, the Moscow branch of the Main Directorate for Moscow, Dmitry Ukhin, for the vertical sampling of soil and ground ice in the extreme conditions of the north of Yakutia.

Author Contributions: Conceptualization: A. G. Sh. and A. M. Ch.; Methodology, A. G. Sh., S. W. and A. I. K.; Investigation, all authors; Writing-Original Draft Preparation: A. G. Sh., S. W., A. I. K., A. M. Ch., T. O., A. N. F., L. L. J., J. C.; Writing-Review & Editing, A. G. Sh., A. M. Ch., S. W., A. N. F., T. O., A. I. K., L. L. J., J. C.

Funding: Financial support for this study was provided by Deutsche Forschungsgemeinschaft (DFG grant no. WE4390/7-1) and project IX.127.2.3 (Siberian Branch Russian academy of Sciences). Thaw slump relief analysis was supported by RFBR grants 18-05-60080 and 18-05-60221.

Conflicts of Interest: The authors declare no conflict of interest.

References

1. Kunitsky, V.V.; Syromyatnikov, I.I.; Schirrmeister, L.; Skachkov, Y.B.; Grosse, G.; Wetterich, S.; Grigoriev, M.N. Ice rocks and thermal denudation near Batagai (Yanskoye plateau, Eastern Siberia). *Earth Cryosphere* **2013**, 17, 56–68 (in Russian).
2. Günther, F.; Grosse, G.; Wetterich, S.; Jones, B.M.; Kunitsky, V.V.; Kienast, F.; Schirrmeister, L. The Batagay mega thaw slump, Yana Uplands, Yakutia, Russia: permafrost thaw dynamics on decadal time scale. PAST Gateways – Palaeo-Arctic Spatial and Temporal Gateways: Third International Conference and Workshop, Potsdam, Germany, 18–22 May 2015, pp. 45–46.
3. Vadakkedath, V.; Zawadzki, J.; Przezdziecki, K. Multisensory satellite observations of the expansion of the Batagaika crater and succession of vegetation in its interior from 1991 to 2018. *Environmental Earth Sciences* **2020**, 79, 150, 1–10.
4. Zhurlov, O.S.; Grudinin, D.A.; Yakovlev, I.G. Phylogenetic 16S metagenomic analysis and antibiotic resistance of psychrotolerant bacteria isolated from the soil of the Batagai failure. *International Journal of Applied and Basic Research* **2015**, 11, 648–651 (in Russian).
5. Opel, T.; Murton J.B.; Wetterich, S.; Meyer, H.; Ashastina, K.; Günther, F.; Grotheer, H.; Mollenhauer, G.; Danilov, P.P.; Boeskorov, V.; Savvinov, G.N.; Schirrmeister, L. Past climate and continentality inferred from ice wedges at Batagay megaslump in the Northern Hemisphere's most continental region, Yana Highlands, interior Yakutia. *Climate of the Past* **2019**, 15, 1443–1461.
6. Murton, J.B.; Edwards, M.E.; Lozhkin, A.V.; Anderson, P.M.; Savvinov, G.N.; Bakulina, N.; Bondarenko, O.V.; Cherepanova, M.V.; Danilov, P.P.; Boeskorov, V.; Goslar, T.; Grigoriev, S.; Gubin, S.V.; Korzun, J.A.; Lupachev, A.V.; Tikhonov, A.; Tsygankova, V.I.; Vasilieva, G.V.; Zanina, O.G. Preliminary paleoenvironmental analysis of permafrost deposits at Batagaika megaslump, Yana Uplands, northeast Siberia. *Quaternary Research* **2017**, 87, 314–330.
7. Wetterich, S.; Murton, J.B.; Toms, P.; Wood, J.; Blinov, A.; Opel, T.; Fuchs, M.C.; Merchel, S.; Rugel, G.; Gärtner, A.; Savvinov, G. Multi-method dating of ancient permafrost of the Batagay megaslump, East Siberia, EGU General Assembly 2020, Online, 4–8 May 2020, EGU2020-2999.
8. Kienast, F.; Ashastina, K.; Troeva, E. Phylogeography of a west-Beringian endemic plant: An ancient seed of Stellaria jacutica Schischk. detected in permafrost deposits of the last interglacial. *Review of Palaeobotany and Palynology* **2018**, 259, 48–54.
9. Melchinov, V.P.; Pavlov, A.A.; Kladkin, V.P.; Bashkuev, Y.B.; Haptanov, V.B. Radio wave diagnostics of ice rocks in the zone of thermokarst failure (Batagai, Yakutia). Proceedings of the XXVI All-Russian Open Scientific Conference, Kazan, Russian Federation, July 01–06, 2019; Kazan (Volga) Federal University Publishing House, 2019,Vol. 1, pp. 495–498 (in Russian).
10. Vasilchuk, Y.K.; Vasilchuk, D.Y.; Budantseva, N.A.; Vasilchuk, A.K.; Trishin, A.Y. High-Resolution Oxygen Isotope and Deuterium Diagrams for Ice Wedges of the Batagai Yedoma, Northern Central Yakutia. *Doklady Earth Sciences* **2019**, 487, 986–989.
11. Vasilchuk, Y.K.; Vasilchuk, J.Y.; Budantseva, N.A.; Vasilchuk, A.C.; Trishin, A.Y. Isotopic and geochemical features of the Batagaika yedoma (preliminary results). *Arctic and Antarctic* **2017**, 3, 69–96 (in Russian).
12. Ashastina, K.; Kuzmina, S.; Rudaya N.; Troeva, E.; Schoch, W.; Römermann, C.; Reinecke, J.; Otte, V.; Savvinov, G.; Wesche, K.; Kienast, F. Woodlands and steppes: Pleistocene vegetation in Yakutia's most continental part recorded in the Batagay permafrost sequence. *Quaternary Science Reviews* **2018**, 196, 38–61.
13. Fedorov, A.N.; Konstantinov, P.Y.; Vasilyev, N.F.; Shestakova, A.A. The influence of boreal forest dynamics on the current state of permafrost in Central Yakutia. *Polar Science*

2019, 22, 100483.
14. Knorre, A.A.; Kirdyanov, A.V.; Prokushkin, A.S.; Krusic, P.J.; Büntgen, U. Tree ring-based reconstruction of the long-terminfluence of wildfires on permafrost active layer dynamics in Central Siberia. *Science of the Total Environment* **2019**, 652, 314–319.
15. Karelin, D.V.; Zamolodchikov, D.G.; Gilmanov, T.G. Reserves and carbon production in the phytomass of tundra and forest-tundra ecosystems of Russia. *Forestry* **1995**, 5, 29–36 (in Russian).
16. Chestnykh, O.V.; Zamolodchikov, D.G.; Utkin, A.I. General reserves of bioremediation of carbon and nitrogen in the soil of the forest fund of Russia. *Russian Forest Sciences* **2004**, 4, 30–42 (in Russian).
17. Hugelius, G.; Strauss, J.; Zubrzycki, S.; Harden, J.W.; Schuur, E.A.G.; Ping, C.-L.; Schirrmeister, L.; Grosse, G.; Michaelson, G.J.; Koven, C.D.; O'Donnell, J.A.; Elberling, B.; Mishra, U.; Camill, P.; Yu Z.; Palmtag, J.; Kuhry, P. Estimated stocks of circumpolar permafrost carbon with quantified uncertainty ranges and identified data gaps. *Biogeosciences* **2014**, 11, 6573–6593.
18. Schepashchenko, D.G.; Mukhortova, L.V.; Shvidenko, A.Z.; Vedrova, E.F. Reserves of organic carbon in the soils of Russia. *Soil Science* **2013**, 2, 123–132 (in Russian).
19. Schuur, E.A.G.; McGuire, A.D.; Schädel, C.; Grosse, G.; Harden, J.W.; Hayes, D.J.; Hugelius, G.; Koven, C.D.; Kuhry, P.; Lawrence, D.M.; Natali, S.M.; Olefeldt, D.; Romanovsky, V.E.; Schaefer, K.; Turetsky, M.R.; Treat, C.C.; Vonk, J.E. Climate change and the permafrost carbon feedback. *Nature* **2015**, 520, 171–179.
20. Masyagina, O.V.; Menyailo, O.V. The impact of permafrost on carbon dioxide and methane fluxes in Siberia: A meta-analysis. *Environmental Research* **2020**, 182, 109096.
21. Gvozdetsky, N.A.; Mikhailov, N.I. Physical geography of the USSR (Asian part); Publisher: Geografgiz, Moscow, 1963; 572 p. (in Russian).
22. Isachenko, A.G. Landscapes of the USSR; Publisher: Leningrad University Publishing house, Leningrad, 1985; 320 p. (in Russian).
23. Danilov, I.D. The permafrost zone of the Earth and its zoning. Bulletin of the USSR Academy of Sciences, *Geographical Series* **1983**, 1, 12–18 (in Russian).
24. Krylenkov, V.A.; Goncharov, A.E. Microbiota of the terrestrial cryosphere; Publisher: Foliant, St. Petersburg, 2019; 448 p. (in Russian).
25. Vincent, W.F. Microbial ecosystem responses to rapid climate change in the Arctic. *The International Society of Microbial Ecology* **2010**, 4 (9), 1087–1090.
26. Graham, D.E.; Wallenstein, M.D.; Vishnivetskaya, T.A.; Waldrop, M.P.; Phelps, T.J.; Pfiffner, S.M.; Onstott, T.C.; Whyte, L.G.; Rivkina, E.M.; Gilichinsky, D.A.; Elias, D.A.; Mackelprang, R.; VerBerkmoes, N.C.; Hettich, R.L.; Wagner, D.; Wullschleger, S.D.; Jansson, J.K. Microbes in thawing permafrost: the unknown variable in the climate change equation. *The International Society of Microbial Ecology* **2012**, 6 (4), 709–712.
27. Nikrad, M.P.; Kerkhof, L.J.; Häggblom, M.M. The subzero microbiome: microbial activity in frozen and thawing soils. *FEMS Microbiology Ecology* **2016**, 92, fiw081.
28. Bazilevich, N.I. Biological productivity of ecosystems of Northern Eurasia; Publisher: Nauka, Moscow, 1993; 293 p. (in Russian).
29. Prokushkin, A.S.; Hagedorn, F.; Pokrovsky, O.S.; Viers, J.; Kirdyanov, A.V.; Masyagina, O.V.; Prokushkina, M.P.; McDowell, W.H. Permafrost regime affects the nutritional status and productivity of larches in Central Siberia. *Forests* **2018**, 9 (6), 314.
30. Shpedt, A.A.; Ligaeva, N.A.; Emelyanov, D.V. Transformation of soil and land resources of the Middle Siberia in the conditions of climatic changes. IOP Conference Series: Earth and Environmental Science, Krasnoyarsk, Russian Federation, 20–22 June 2019, 315, 052051 (in Russian).
31. Ashastina, K.; Schirrmeister, L.; Fuchs, M.; Kienast, F. Palaeoclimate characteristics in

interior Siberia of MIS 6-2: first insights from the Batagay permafrost mega-thaw slump in the Yana Highlands. *Climate of the Past* **2017**, 13, 795–818.